ISSN: 1813-4890

Mechanical analysis of inner ring mass unbalance rolling bearing based on LS-DYNA

Ruigang Lu [a], Kun Ni [b], Mengjiao Lv [c], Fa Zhou [d]

School of Qingdao University of Technology, Qingdao 266520, China

[a]519190901@qq.com, [b]1626896008@qq.com, [c]1850854998@qq.com, [d]2293566131@qq.com

Abstract

Rolling bearings are important supporting components in the manufacturing industry for rotating machinery, with advantages such as low friction resistance, high speed, and compact structure. During the actual operation of rolling bearings, deformation occurs at the contact between the rolling elements and the raceways, causing the load borne by the rolling elements to change with their deformation, thereby affecting the normal operation of the entire rotating mechanism. Eccentricity faults in the inner ring of bearings can alter the contact state between the inner ring and the rolling elements, affecting the deformation of the rolling elements and ultimately leading to bearing failure or accelerated bearing failure. For bearings with inner ring mass unbalance faults, a model of inner ring mass unbalance rolling bearings is established to analyze the impact of centrifugal forces generated on the inner ring on the performance of bearings. The study investigates the stress distribution of rolling bearings under different speeds and mass conditions, as well as their effects on the contact characteristics of internal components within the bearings and the operational status. Explanations are provided for the reasons behind changes in the contact of internal components in bearings with mass unbalance faults.

Keywords

Cylindrical roller bearings; mass unbalance;LS-DYNA.

1. Introduction

With the continuous advancement of intelligent manufacturing and the "Industry 5.0" process, the requirements for high precision, high performance, and long life are driving China's industrial equipment manufacturing technology and theory towards higher levels of breakthroughs and innovations. Localized faults are one of the two main categories of bearing failures, including cracks, pits, spalling, dents, and surface roughness on various components of rolling element bearings. Bearing cracks include surface cracks and subsurface cracks. Subsurface cracks most commonly occur in the maximum shear stress zone below the surface of the bearing components. Yoshioka and Fujiwara developed acoustic emission and vibration acceleration methods to diagnose the initiation and propagation time of rolling contact fatigue cracks, which can provide the initial crack propagation time and propagation time of fatigue cracks. Mano et al. proposed a new method for acoustic emission source localization based on experimental and simulation methods for predicting the relationship between radial rolling contact fatigue crack propagation and inner ring load distribution in radial rolling bearings. This is the narrow zone of initial fatigue crack propagation. Tandon and Choudhury established an analytical model to predict the vibration of rolling bearings with spalling on rolling components and raceways under axial and radial loads. The model considers the influence of load and pulse shape on vibration amplitude, as well as the finite width pulse caused by faults.

ISSN: 1813-4890

In this model, three typical pulse forms are defined: rectangular, triangular, and semicircular. Kiral and Karaglle used the finite element method to predict the effect of speed, shell structure geometry, number and location of faults on the frequency domain vibration of single and multiple fault raceways and rolling elements in rolling bearings. Aithal et al. established a static finite element model to study the impact of surface roughness error on the load distribution of large-diameter rotary bearings used in fast neutron breeding reactor rotating plugs. They demonstrated that the amplitude of the roughness has a significant impact on the load distribution of the bearing. Xing et al. established an analytical model to predict the vibration and surface roughness of SRBs. External axial loads and automatic aligning contact angles are formulated in their model.

2. Mass eccentricity

2.1. Modeling of eccentric rolling bearing with inner ring mass

The mass point is divided into four cases: 0g (normal bearing), 0.1g, 10g, and the mass point is located at the middle node of the inner ring, as shown in Figure 1. At the same time, the rotating speed is 3000rpm and the external load Q is 1000N. The calculation is 0.1s and 1000 steps are output, which takes 56h.

Different from the research method of geometric eccentric fault, in order to reduce the influence of external load on bearing, the motion trend of node X direction on bearing components is selected in this section for analysis.

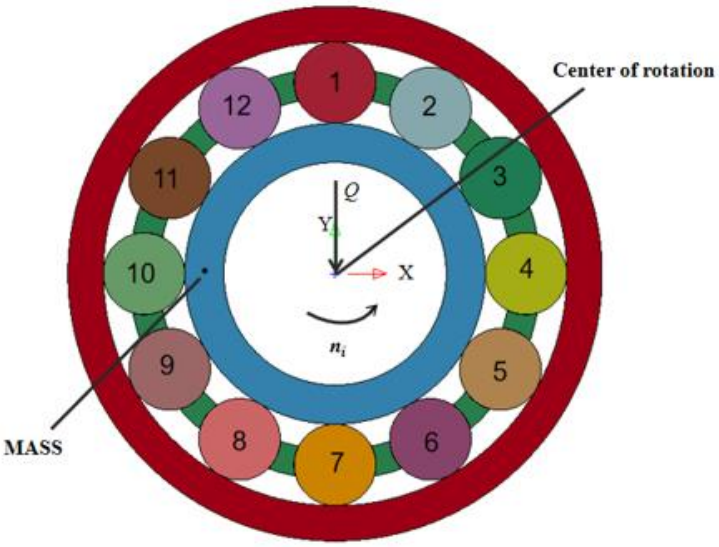

Fig1.Mass point inner circle position diagram

2.2. Influence of eccentric mass on rolling bearing

(1) At the same speed, the displacement and speed time history analysis of each component of the inner ring mass eccentric bearing

ISSN: 1813-4890

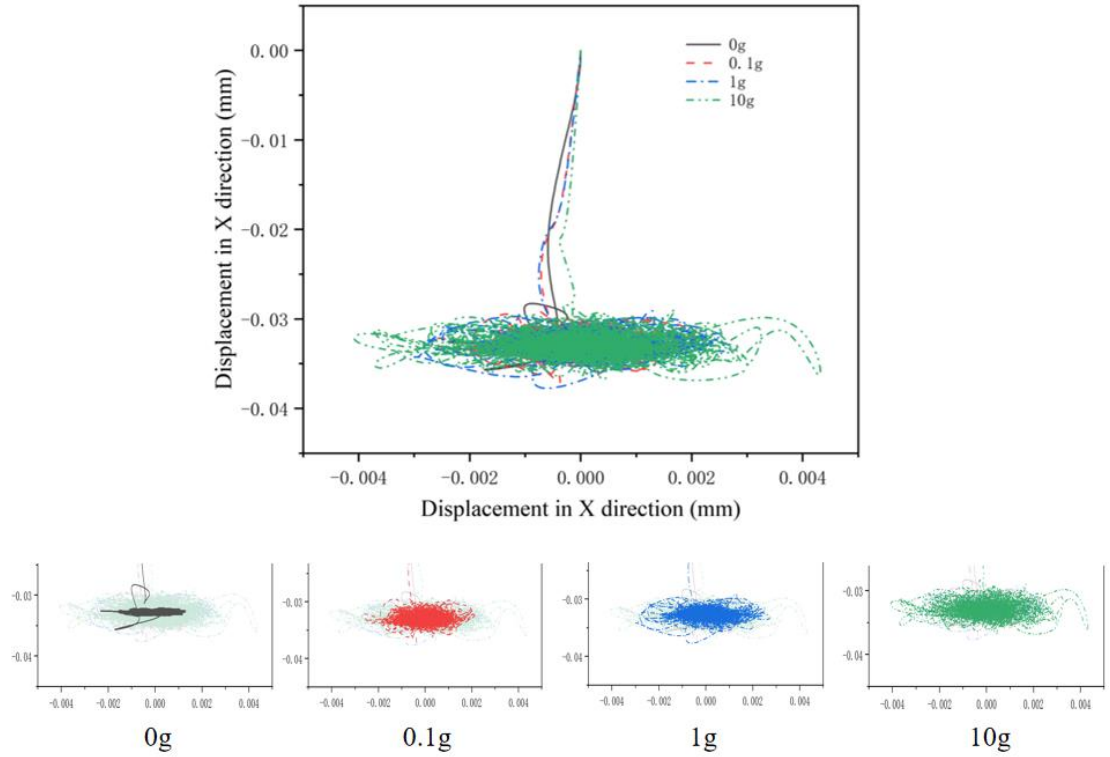

Fig2.Center track curve of inner ring of rolling bearing with different eccentric mass

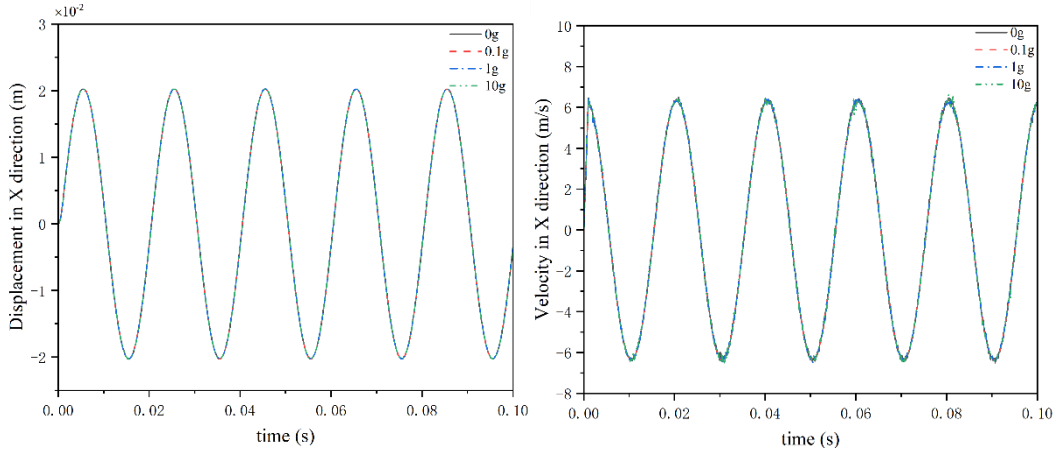

(a).X displacement velocity curve of inner ring node of rolling bearing with different eccentric mass

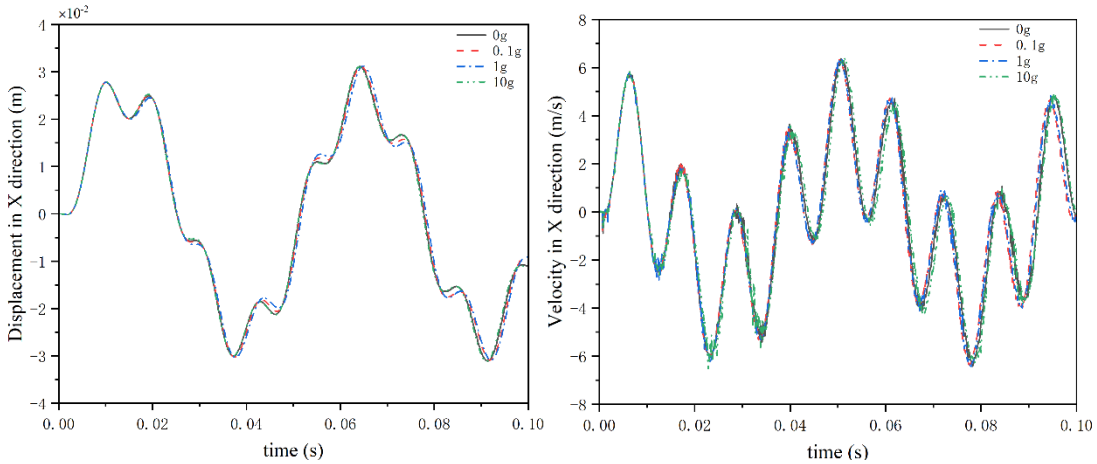

(b).X displacement velocity curve of rolling body segment of rolling bearing with different eccentric mass

ISSN: 1813-4890

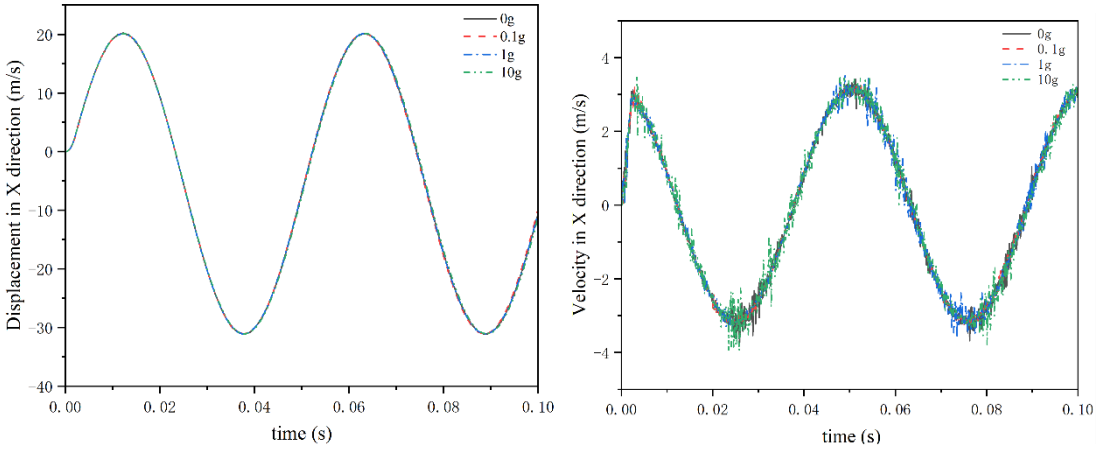

(c).X displacement velocity curve of cage joints of rolling bearing with different eccentric mass

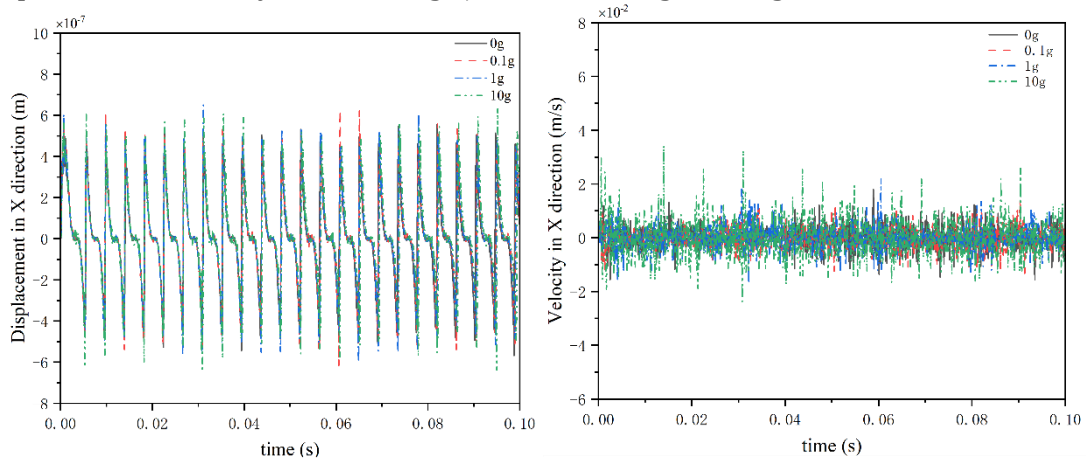

Fig3.Displacement curve in X direction of raceway node of outer ring of rolling bearing with different eccentric mass

It can be seen that the center trajectory of the rolling bearing changes with the increase of eccentric mass. The larger the mass is, the larger the displacement trajectory range of the center of the inner ring, and the larger the displacement vibration amplitude of the inner ring of the rolling bearing.

By analyzing the displacement curves of each component of the mass eccentric rolling bearing in Fig.3, it can be seen that the inner ring and cage node of the mass eccentric bearing basically coincide with the inner ring and cage node of the healthy bearing in the X direction, showing the same periodic change, indicating that the displacement of the inner ring and cage in the X direction during operation is little affected by the mass eccentric. The displacement change of rolling node in X direction is much greater than that of inner ring and cage. It can be seen from the speed curve that the X direction velocity of the node on the inner ring basically coincides with that of the healthy bearing inner ring node. When the inner ring node rotates to the farthest point in the X direction, the speed curve of the inner ring node fluctuates. According to the contact relationship between the internal components of the bearing, the speed of the rolling element and the cage also changes.

ISSN: 1813-4890

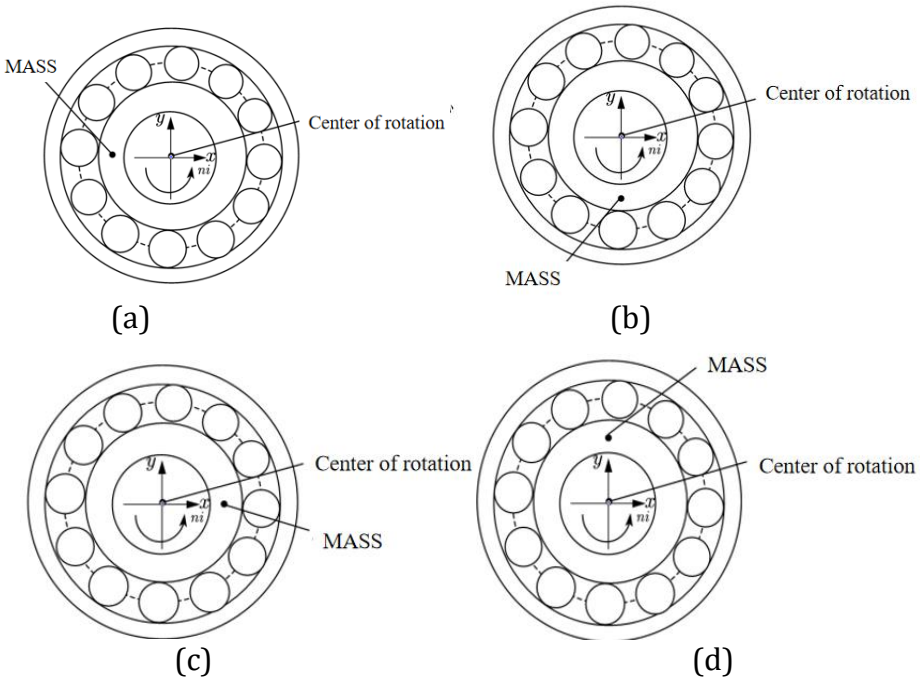

Fig4.Equivalent stress cloud diagram of mass eccentric rolling bearing at the same speed and different time

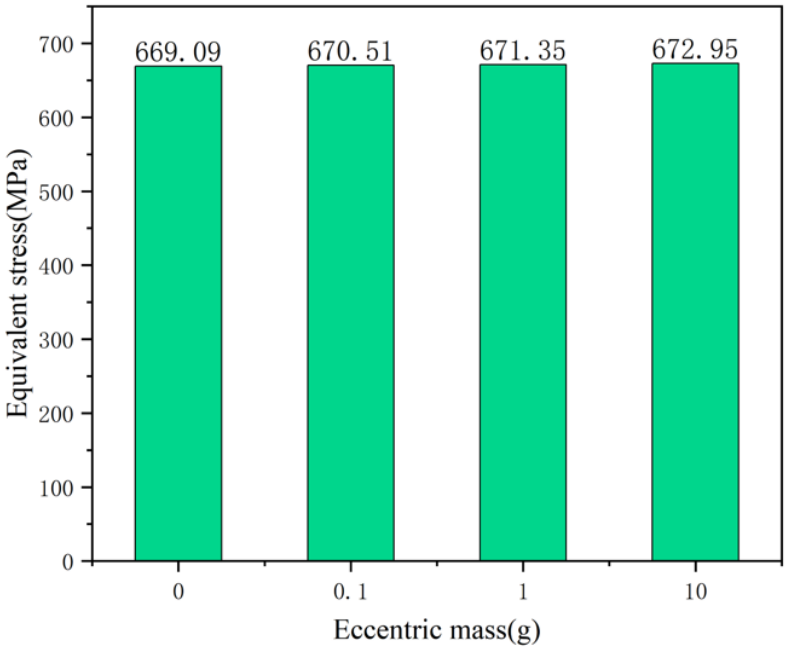

Fig5. Comparison of average maximum equivalent stress of rolling bearing at the same speed

It can be seen from Fig4 that the bearing area of the bearing with mass eccentric fault at different times is similar to that of the healthy bearing, both of which are below the bearing. Different from the equivalent stress distribution of the healthy bearing, the bearing has a phenomenon of stress concentration at the mass point of the inner ring during the running process, which is more obvious in Fig.4(a). The maximum value of the equivalent stress occurs in the contact area between the rolling element and the inner ring. The number of rolling elements in the bearing zone changes with the rotation of the inner ring, and the number of rolling elements in the bearing zone is 4 to 5.

As shown in Figure 5, when the mass point is rotated five times to the bottom of the inner ring, the average maximum equivalent stress of the healthy rolling bearing is 669.09MPa; When the mass eccentricity is 0.1g, the average maximum equivalent stress of rolling bearing is

ISSN: 1813-4890

670.51MPa. When the mass eccentricity is 1g, the average maximum equivalent stress of the rolling bearing is 671.35MPa. When the mass eccentricity is 10g, the average maximum equivalent stress of the rolling bearing is 672.95MPa. The equivalent stress of rolling bearing increases with the increase of eccentric mass.

3. Effect of rotational speed on mass eccentric fault bearing

In order to achieve more accurate results, the eccentric mass is 10g, the external load is Q=1000N, and only the bearing speed is changed, which is divided into the following cases: the speed is 3000rpm, 4000rpm, 6000rpm.

(1) Displacement and speed time history analysis of mass eccentric rolling bearing components at different speeds

In order to obtain accurate steady-state simulation data within a limited time, the simulation results of a model with rotational speed of 3000rpm, 4000rpm, 6000rpm, mass of 10g and external load of 1000N were selected for analysis.

As can be seen from Fig 6. center track of mass eccentric bearing inner ring, with the increase of rotational speed, the range of center motion track of bearing inner ring also increases correspondingly, gradually showing an irregular circular region. When the rotation speed is 6000rpm, the orbit of the center of the circle shows an oblate circle.

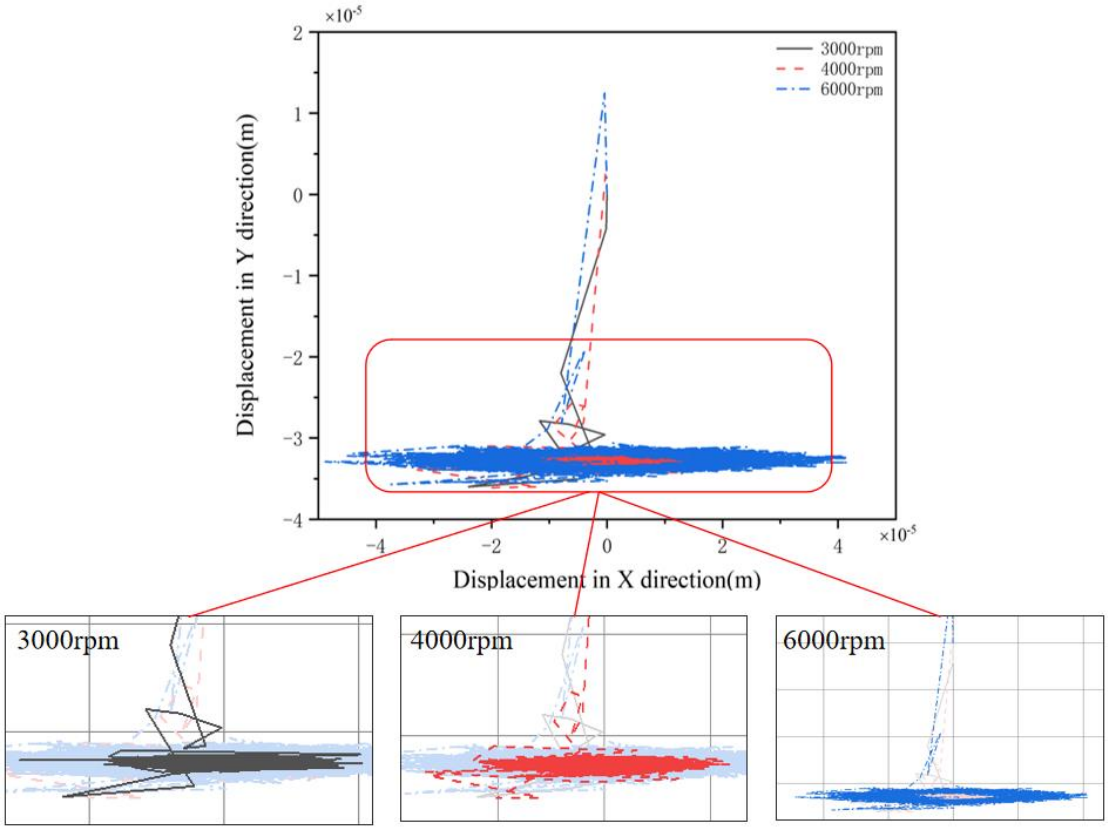

Fig6. Orbit curve of mass eccentric bearing inner ring at different speed

From Fig.7(a) to (c) displacement curves, it can be seen that under the same eccentric mass, different rotational speeds have little influence on the displacement of the bearing inner ring, rolling element and cage in the X direction. The displacement curve of the three bearings in the X direction is the same as that of normal rolling bearings, showing periodic changes, and the displacement period also decreases with the increase of rotational speed. The period of the velocity curve and the displacement curve in the X direction of the inner ring and the cage node is close to that of the inner ring. When the velocity reaches the maximum, the displacement also reaches the maximum. It can be seen from the speed curve that under different speed, the speed

ISSN: 1813-4890

trend on each bearing component is the same as that in the upper section, and the maximum node speed on the inner ring is the largest, followed by the rolling node speed, and finally the cage speed is the smallest.

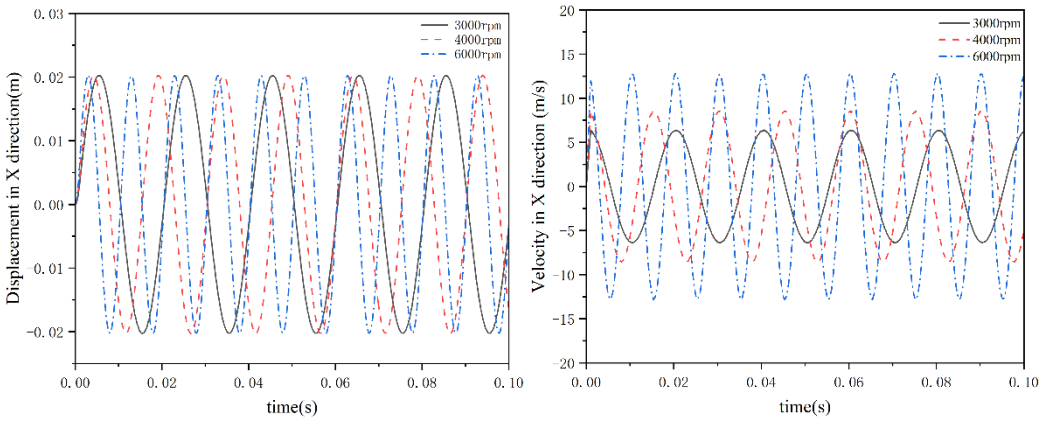

(a) Displacement and velocity curve of mass eccentric bearing inner ring node in X direction at different speed

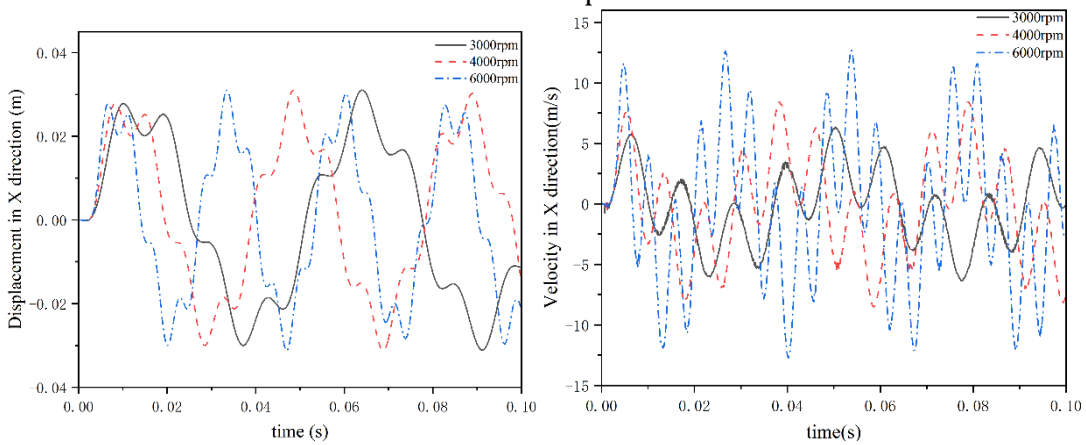

(b)Displacement and velocity curve of mass eccentric bearing rolling node in X direction at different speed

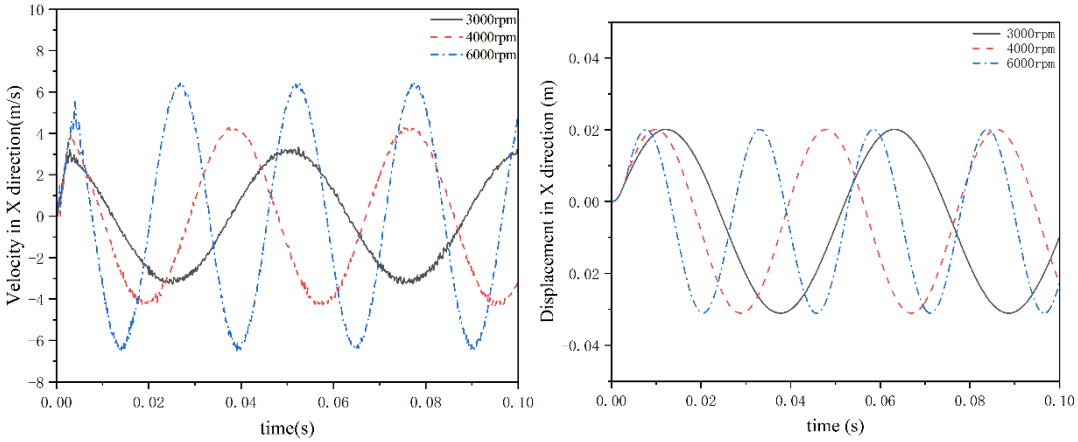

(c)Displacement and velocity curve of mass eccentric bearing cage node in X direction at different speed

Fig7.Displacement velocity curve in X direction of nodes of mass eccentric rolling bearing at different speed

As can be seen from Figure 8, the X-direction displacement of node 9328 in the outer ring presents a periodic change, and with the increase of rotational speed, the maximum

ISSN: 1813-4890

displacement in the X-direction will also increase. The speed of the outer ring node in the X direction also increases with the increase of the rotational speed.

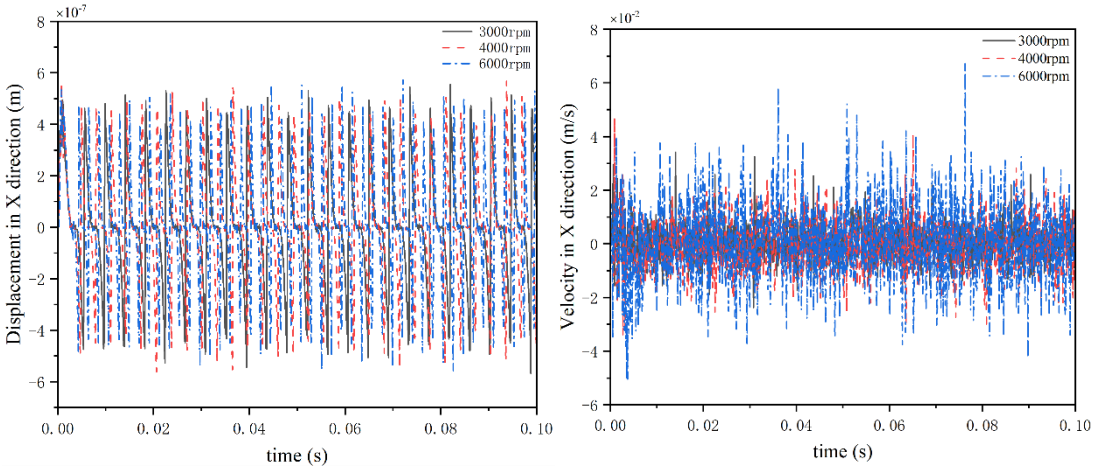

Fig8.Comparison of displacement velocity in X direction of mass eccentric outer ring No. 9328 node under different rotation speeds

4. Conclusion

In this chapter, finite element models of geometric eccentric and mass eccentric rolling bearings are established, dynamic simulation is carried out for these two kinds of faulty bearings, and the law of equivalent stress, displacement and velocity change of each component of eccentric rolling bearings is analyzed, and the following conclusions are obtained:

In the case of mass eccentric fault bearings, the same speed and different eccentric mass, the centrifugal force generated by the inner ring of the rolling bearing makes the contact force between the rolling body and the outer ring raceway different. When the mass point on the inner ring moves below the center of the inner ring, under the action of centrifugal force, the contact force between the rolling element in the bearing zone and the raceway will slightly increase with the increase of eccentric mass. When the mass point on the inner ring moves above the center of the inner ring, the contact force between the rolling element in the bearing zone and the raceway will decrease slightly with the increase of the eccentric mass.

At different speeds, in bearings with the same eccentric mass, when the rolling body is in the bearing area and the mass is just below the center of the inner circle, the peak value of the contact force on the same rolling body increases with the increase of the rotating speed; When the rolling body is in the bearing area and the mass is just above the center of the inner circle, the peak value of the contact force on the same rolling body decreases slightly with the increase of the rotational speed. The equivalent stress distribution of mass eccentric fault bearings is similar to that of healthy bearings and does not change with the rotation of the inner ring. The faster the speed, the greater the various effects of mass eccentricity on the bearing

Acknowledgements

The authors declared no potential conflicts of interest with respect to the research, authorship, and/or publication of this article. The authors thank Qingdao University of Technology and Shandong Jiao tong University for the support and contribution.

Funding: This work was supported by the National Natural Science Foundation of China (grant number 52202508); the Key Lab of Industrial Fluid Energy Conservation and Pollution Control, Ministry of Education (grant number 2022-JXGCKFKT-YB-04); the Key Laboratory of Transportation Industry for Transport Vehicle Detection, Diagnosis and Maintenance Technology (grant number JTZL2202).

ISSN: 1813-4890

References

[1] Lou, Han, Liu, et al.The rolling contact fatigue behaviors in carburized and hardened steel. In: Kitagawa, H., Tanaka, T. (eds.) Fatigue 90: Proceedings of the Fourth International Conference on Fatigue and Fatigue Thresholds, pp.1990, July, 627–632. Honolulu, HI.

[2] Saheta, V.Dynamics of Rolling Element Bearings Using Discrete Element Method. M.S. Thesis, Purdue University, 2001,West Lafayette.

[3] WassgrenR C ,Professor A,SadeghiF , et al.Cage Instabilities in Cylindrical Roller Bearings[J].Journal of Tribology,2004,126(4):681-689.

[4] Yoshioka, T, Fujiwara.Measurement of propagation initiation and propagation time of rolling contact fatigue cracks by observation of acoustic. Tribol. Ser.1987, 12, 29-33

[5] Mano, H., Yoshioka, T., Korenaga, A., et al.Relationship between growth of rolling contact fatigue cracks and load distribution. Tribol. Trans. 2000,43(3), 367–376

[6] Tandon and A. Choudhury. AN ANALYTICAL MODEL FOR THE PREDICTION OF THE VIBRATION RESPONSE OF ROLLING ELEMENT BEARINGS DUE TO A LOCALIZED DEFECT[J]. Journal of Sound and Vibration, 1997, 205(3) : 275-292

[7] Kiral Z ,Karagülle H.Simulation and analysis of vibration signals generated by rolling element bearing with defects[J].Tribology International,2003,36(9):667-678.

[8] Kıral Z ,Karagülle H.Vibration analysis of rolling element bearings with various defects under the action of an unbalanced force[J].Mechanical Systems and Signal Processing,2005,20(8):1967-1991.

[9] Sriramachandra Aithal;N Siva Prasad;MS Shunmugam;et al.Effect of manufacturing errors on load distribution in large diameter slewing bearings of fast breeder reactor rotatable plugs[J].Proceedings of the Institution of Mechanical Engineers, Part C: Journal of Mechanical Engineering Science,2016,Vol.230(9): 1449-1460

[10] Xing, Y (Xing, Yu); Xu, Hua;et al.Mechanical analysis of spherical roller bearings due to misalignments between inner and outer rings[J].PROCEEDINGS OF THE INSTITUTION OF MECHANICAL ENGINEERS PART C-JOURNAL OF MECHANICAL ENGINEERING SCIENCE,2017, Vol.231 (17): 3250-3262